

TLQP Peptides in Amyotrophic Lateral Sclerosis: Possible Blood Biomarkers with a Neuroprotective Role

Carla Brancia,^{a*} Barbara Noli,^a Marina Boido,^b Roberta Pilleri,^a Andrea Boi,^a Roberta Puddu,^c Francesco Marrosu,^c Alessandro Vercelli,^b Paolo Bongioanni,^d Gian-Luca Ferri^{af} and Cristina Cocco^{af}

^a Dept. Biomedical Sciences, University of Cagliari, Monserrato, Italy

^b Neuroscience Institute Cavalieri Ottolenghi, Dept. Neuroscience, University of Turin, Turin, Italy

^c Dept. Neurology, Azienda Universitario Ospedaliera di Cagliari & University of Cagliari, Cagliari, Italy

^d Neurorehabilitation Unit, Dept. Neuroscience, University of Pisa, Pisa, Italy

Abstract—While the VGF-derived TLQP peptides have been shown to prevent neuronal apoptosis, and to act on synaptic strengthening, their involvement in Amyotrophic Lateral Sclerosis (ALS) remains unclarified. We studied human ALS patients' plasma (taken at early to late disease stages) and primary fibroblast cultures (patients vs controls), in parallel with SOD1-G93A transgenic mice (taken at pre-, early- and late symptomatic stages) and the mouse motor neuron cell line (NSC-34) treated with Sodium Arsenite (SA) to induce oxidative stress. TLQP peptides were measured by enzyme-linked immunosorbent assay, in parallel with gel chromatography characterization, while their localization was studied by immunohistochemistry. In controls, TLQP peptides, including forms compatible with TLQP-21 and 62, were revealed in plasma and spinal cord motor neurons, as well as in fibroblasts and NSC-34 cells. TLQP peptides were reduced in ALS patients' plasma starting in the early disease stage (14% of controls) and remaining so at the late stage (16% of controls). In mice, a comparable pattern of reduction was shown (vs wild type), in both plasma and spinal cord already in the pre-symptomatic phase (about 26% and 70%, respectively). Similarly, the levels of TLQP peptides were reduced in ALS fibroblasts (31% of controls) and in the NSC-34 treated with Sodium Arsenite (53% of decrease), however, the exogeneous TLQP-21 improved cell viability (SA-treated cells with TLQP-21, vs SA-treated cells only: about 83% vs. 75%). Hence, TLQP peptides, reduced upon oxidative stress, are suggested as blood biomarkers, while TLQP-21 exerts a neuroprotective activity. © 2018 Published by Elsevier Ltd on behalf of IBRO.

Key words: TLQP-peptides, neurodegeneration, ALS, motor neurons, NSC-34 cells, human fibroblasts.

INTRODUCTION

Amyotrophic Lateral Sclerosis (ALS) is a progressive neurodegenerative disease characterized by neuronal degeneration in frontal cortex, brainstem and spinal cord. Virtually all muscles are gradually affected, with difficulties in speaking, swallowing and breathing, and

death ensues 3–5 years after appearance of the first symptoms. Currently, no treatment is effective in stopping the progression of the disease, nor is any early diagnostic test available. While the etiology of ALS is unknown, mutations of the superoxide dismutase 1 (SOD1) gene, or of the TARDBP (TAR DNA Binding Protein) gene have been hypothesized as common causes (Chiò et al., 2011; Zarei et al., 2015). In fact, oxidative stress, characterized by an altered equilibrium between the production of reactive oxygen species (free radicals) and antioxidant reactions, has been related to motor neuron degeneration in ALS (Bergeron, 1995; Robberecht, 2000). TLQP peptides are a family of peptides derived from the VGF (non acronymic) precursor protein, some of these originally identified in rat brain (Trani et al., 2002). They share a common N-terminal “TLQP” (Thr-Leu-Gln-Pro) amino acid sequence, are cleaved from the primary VGF product at the specific R-P-R (Arg-Pro-Arg) processing site found at rat/mouse VGF_{553–555} (VGF_{551–553} in human), and variably extend

*Corresponding author. Address: NEF Lab, Dept. Biomedical Science, Cittadella Univers. 1, 09042 Monserrato, CA, Italy.

E-mail address: cbrancia@unica.it (C. Brancia).

† Co-senior authors.

Abbreviations: ALS, Amyotrophic Lateral Sclerosis; ALSFRS-R, ALS Functional Rating Scale-Revised; C3AR, complement component 3a receptor 1; gC1q-R, receptor for the globular heads of c1q; DMEM, Dulbecco's modified Eagle's medium; EDTA, ethylenediaminetetraacetic acid; ELISA, enzyme-linked immunosorbent assay; ER, endoplasmic reticulum; MTT, 3-(4,5-Dimethylthiazol-2-yl)-2,5-Diphenyltetrazolium Bromide; NSC-34, mouse motor neuron-like hybrid cell line; PBS, phosphate-buffered saline; PIC, protease inhibitor cocktail; PFA, paraformaldehyde; SA, Sodium Arsenite; SOD1, superoxide dismutase 1; VACHT, vesicular acetylcholine transporter; TARDBP, TAR DNA-Binding Protein.

to the VGF precursor C-terminus (Brancia et al., 2010). In the brain, TLQP peptides appear to show a restricted localization compared to other VGF-derived peptides, including a subpopulation of hypothalamic neurons projecting to a discrete area of median eminence (Brancia et al., 2010; Noli et al., 2014). Recently, a differential expression of several TLQP peptides was reported in the Syrian hamster brain. Namely, TLQP-21 (21 amino acid in length, rat VGF_{556–576}) was well represented in both hypothalamus and cortex while the longer form of TLQP-62 (rat VGF_{556–617} encompassing the VGF precursor's C-terminus) was abundant in cortex, and less expressed in hypothalamus (Noli et al., 2015). TLQP peptides were also found in hypothalamic–pituitary axis and plasma, differently expressed during the oestrous cycle phases (Noli et al., 2014) as well as in several peripheral locations including adrenal and stomach, changing in condition of stress and upon fasting, respectively (D'Amato et al., 2008; Brancia et al., 2010). Additional molecular forms compatible with predicted TLQP-30 and TLQP-42 peptides were revealed in certain endocrine organs (Cocco et al., 2007; Brancia et al., 2010) but have not been further studied so far. In human plasma, TLQP peptides were upregulated upon hyperglycemia, and downregulated in obese subjects (D'Amato et al., 2015). As to bioactivity and possible role/s, TLQP-21 has been shown to be involved in the regulation of metabolic mechanisms (Bartolomucci et al., 2006; Jethwa et al., 2007; Lewis et al., 2017), reproduction (Aguilar et al., 2013; Noli et al., 2014), chronic stress (Razzoli et al., 2012) and inflammatory pain (Rizzi et al., 2008). The same peptide prevented apoptosis of rat cerebellar granules upon serum and potassium deprivation, with modulation of kinase phosphorylation (Severini et al., 2008). Also, it protected human umbilical vein endothelial cells against high-glucose-induced apoptosis, by enhancing glucose-6-phosphate dehydrogenase and nicotinamide adenine dinucleotide phosphate dehydrogenase, hence reducing reactive oxygen species (Zhang et al., 2013). Two receptor molecules have been identified for TLQP-21, namely the complement component 3a receptor (C3a-R: Hannedouche et al., 2013; Cero et al., 2014, 2016) and the receptor for the globular heads of c1q (gC1q-R: Chen et al., 2013) and involved, with TLQP-21, in modulating lipolysis (Cero et al., 2016) and neuropathic pain (Chen et al., 2013), respectively. While the precise mechanisms involved are not entirely known, there is strong evidence that the TLQP-21 may act by increasing intracellular calcium in Chinese hamster ovary cells (Cassina et al., 2013), microglia (Chen et al., 2013) and cerebellum (Severini et al., 2008). The longer form of TLQP-62 has been widely investigated in hippocampus where it enhances synaptogenesis (Behnke et al., 2017), regulates memory formation, and induces both synaptic potentiation (Bozdagi et al., 2008; Lin et al., 2015) and neurogenesis (Thakker-Varia et al., 2014). It can also cause dorsal horn cell hyper-excitability and behavioral hypersensitivity in rats (Moss et al., 2008). No specific receptor has been identified so far for TLQP-62. In ALS, despite the reported evidence that VGF expression is modulated in the animal model and humans (Pasinetti

et al., 2006; Zhao et al., 2008), limited information is available regarding TLQP peptides. We have previously reported the involvement of the VGF C-terminal peptides in ALS, modulated in the SOD1 mutant mice and patient's plasma, but exclusively at the final disease phase (Brancia et al., 2016). Afterward, we aimed at specifically investigating the role of the TLQP peptides in ALS, by studying their expression and changes (using ELISA and immunohistochemistry) in transgenic mice (SOD1-G93A) and the mouse motor neuron-like hybrid cell line (NSC-34), as experimental models. In parallel, we also investigated, by ELISA, ALS patients' plasma and primary fibroblast cultures, the latter being considered a good cellular model used in human ALS research (Sabatelli et al., 2015; Yang et al., 2015) and also, contain VGF (Brancia et al., 2016). Moreover, in the NSC-34 cells, the neuroprotective role of the TLQP-21 was addressed in parallel with the presence of its two known receptors (gC1q-R and C3a-R), examined by both western blot and immunocytochemistry.

EXPERIMENTAL PROCEDURES

Human subjects

Subjects of Sardinian descent were studied, including ALS patients (females: $n = 20$, males: $n = 24$, age range: 25–85 yrs), and age-matched controls (unaffected by either neurological conditions, or diabetes; females: $n = 20$, males: $n = 26$). In patients, ALS-related mutations were studied as follows: exon 6 of the TARDBP gene, and all five coding exons of the SOD1 gene were screened by polymerase chain reaction and sequenced using the Big-Dye Terminator v3.1 kit (Applied Biosystems Inc) and an ABI Prism 3130 Genetic Analyzer. A repeat-primed polymerase chain reaction assay was used to screen for the GGGGCC hexanucleotide expansion in the first intron of C9ORF72 (DeJesus-Hernandez et al., 2011; Renton et al., 2011). ALS patients studied showed either: TARDBP-A382T mutation ($n = 16$), SOD1-G93A mutation ($n = 3$); expansion in the C9ORF72 gene ($n = 5$), or no identifiable ALS-related mutation ($n = 20$). The patients' motor and functional (which incorporates additional assessments of dyspnea, orthopnea, and the need for ventilatory support) performance was assessed at the time of blood sampling, by at least two experienced neurologists, according to the ALS Functional Rating Scale Revised (ALSFRS-R: Cedarbaum et al., 1999). Patients' data (summarized in Appendix A: Table 1A), including: age, gender, genetic mutation, ALSFRS-R score and co-morbidity at the time of blood sampling, as well as their clinical condition one year later (whether alive, or not, with or without tracheostomy). On the latter basis, patients were assigned to either group I, "early disease stage" ($n = 25$): patients who were alive and free of tracheostomy one year after blood sampling; or group II, "late disease stage" ($n = 19$): patients who were deceased, or had undergone tracheostomy. The present study was approved by the Ethics Committee at the Cagliari AOU ("Azienda Ospedaliero Universitaria di Cagliari"), protocol n. 450/09/C.E. All patients provided

159 their written informed consent to be part of the study
160 according to the Italian legislation.

161 Human samples

162 Blood samples were collected with
163 ethylenediaminetetraacetic acid (EDTA, 1.5 mg/ml),
164 rapidly centrifuged (14,000 rpm, 5 min), hence plasma
165 was aliquoted and stored frozen (at -80°C). Fibroblast
166 primary cultures were set up using skin biopsies (taken
167 under local anesthesia) obtained from “late disease
168 stage” ALS patients ($n = 4$: two showed a heterozygous
169 missense TARDBP-A382T mutation, two showed no
170 identifiable ALS-related mutation), and age-matched
171 controls ($n = 3$). Cultures were grown as previously
172 reported (Orrù et al., 2016), using high-glucose Dul-
173 becco’s modified Eagle’s medium (DMEM) supplemented
174 with fetal bovine serum (20% vol/vol) and penicillin/strep-
175 tomycin (10 ml/L of: 10,000 U penicillin + 10 mg/ml strep-
176 tomycin in 150 mmol/L NaCl). Oxidative stress was
177 induced adding sodium Arsenite (SA) to the culture med-
178 ium (0.5 mmol/L, for 60 min). For ELISA, cultures were
179 expanded, and four culture plates per patient (or control),
180 and per treatment (SA, or no treatment), were separately
181 extracted in phosphate-buffered saline (PBS: 0.01 mol/L
182 PO_4 , pH 7.2, 0.15 mol/L NaCl) containing a protease inhi-
183 bitor cocktail (PIC, Sigma–Aldrich P8340, 10 ml/g tissue).
184 Remaining extracts (from controls’ explants) were pooled
185 and used for gel chromatography.

186 For immunocytochemistry, cells were grown on
187 coverslips, and at least three coverslips (per
188 patient/control, and per treatment) were fixed in
189 paraformaldehyde (PFA: 40 g/L in PBS, 15 min),
190 permeabilized with cold methanol (5 min), hence Triton
191 X-100 (20 ml/L in PBS, 20 min), and rinsed with PBS.
192 Coverslips were immunostained for TLQP peptides, and
193 with a HuR antibody (Santa Cruz, Antibody Registry:
194 AB627770, raised in mouse, 1:500) to label stress
195 granules, while nuclei were counterstained with
196 bisBenzimide (Hoechst 33342, 0.5 $\mu\text{g/ml}$ in PBS).

197 SOD1-G93A mice

198 Transgenic B6SJL-TgN(SOD1-G93A)1Gur mice were
199 used, over-expressing human SOD1 containing the
200 Gly₉₃ to Ala mutation (Jackson Laboratory, Bar Harbor,
201 ME, USA; stock number 002726; housed at the
202 University of Turin animal house facilities). All
203 experimental procedures on live animals were carried
204 out in accordance with the European Communities
205 Council Directive 86/609/EEC (November 24, 1986),
206 and the Italian Ministry of Health and University of Turin
207 institutional guidelines on animal welfare (law 116/92 on
208 Care and Protection of living animals undergoing
209 experimental or other scientific procedures;
210 authorization number 17/2010-B, June 30, 2010). The
211 Ethics Committee at the University of Turin approved
212 the study. All possible efforts were made to minimize
213 the number of animals used and their suffering. Animal
214 genotyping and behavioral testing used to assess
215 disease progression (neurological test, rotarod and paw
216 grip endurance tests) were previously described in detail

(Boido et al., 2014). Transgenic animals were grouped
according to age (days postnatal: P) and stage of motor
dysfunctions (Brancia et al., 2016), as follows: (i) pre-
symptomatic (around P45); (ii) early-symptomatic (around
P90; two repeated deficits for two consecutive times); (iii)
late-symptomatic (around P120; $\geq 20\%$ weight loss and
inability to perform tests). Age-matched wild-type mice
were used as controls: groups (iv) through (vi), respec-
tively. Male mice were used in all cases, in view of our
previous finding of TLQP modulations in female rodents
along the oestrous cycle (Noli et al., 2014).

For ELISA and gel chromatography, animals ($n = 7$
per group) were anesthetized (3% isoflurane vaporized
in $\text{O}_2/\text{N}_2\text{O}$ 50:50), hence blood was drawn by cardiac
puncture, collected in EDTA-containing tubes (1.78 mg/
ml), and centrifuged (11,000 rpm, 5 min). Plasma was
aliquoted and stored frozen (-80°C). Upon blood
sampling, animals were euthanized by cervical
dislocation, and spinal cords were dissected. Tissues
were coarsely minced with a scalpel, collected in tubes
with ice-cold PBS containing PIC (10 ml/g tissue),
treated with an Ultra-Turrax tissue homogenizer (Ika-
Werke, Staufen, Germany, 3 min), hence tubes were
heated in a vigorously boiling water bath (10 min), and
centrifuged (3000 rpm, 15 min). Supernatants were
stored frozen until use (-20°C). For
immunohistochemistry, mice ($n = 3$ per group) were
anesthetized as above, and perfused transcardially with
PFA (10 min). The whole spinal cord was removed and
post-fixed in PFA (at 4°C , 2 h). Cryosections of cervical
and lumbar spinal cord (8- μm thickness) were
immunostained (in single and double
immunofluorescence) for TLQP peptides, and with an
antibody to vesicular acetylcholine transporter (VACht,
BIOMOL Research lab, Antibody Registry: AB2052813,
raised in goat, 1:400) to label cholinergic motor neurons.

NSC-34 cells and oxidative stress

Cells were grown in high-glucose DMEM, supplemented
with fetal bovine serum (10% vol/vol) and penicillin/
streptomycin (as for fibroblasts, see above). For testing,
cells were plated at a 50,000/ml density in 24-well
plates (24 h), hence underwent oxidative stress by
addition of SA (0.5 mmol/L in culture medium, 60 min at
 37°C) and measured the levels of TLQP-21, NERP-1,
NAPP- and APGH-peptides, as well as VGF N-terminus
and C-terminus. The effect of TLQP-21, NERP-1
(synthetic, custom produced for us by CPC Scientific,
Sunnyvale, CA, USA) was assessed by addition to the
culture media, in the presence/absence of SA, at a
range of concentrations (0.1–10 nmol/ml). Cell
proliferation and viability was assessed used a
colorimetric method based on the 3-(4,5-Dimethylthia-
zol-2-yl)-2,5-Diphenyltetrazolium Bromide reagent (MTT
test, Sigma–Aldrich), according to the manufacturer’s
protocol. Absorbance was measured at 570 nm
(EnVision plate analyzer, Perkin Elmer, Milan, Italy). For
ELISA and gel chromatography, cell preparations were
extracted with PBS containing PIC (10 ml/g tissue), as
described for fibroblasts. For immunocytochemistry,
preparations grown on glass coverslips were fixed with

277 PFA (10 min), permeabilized with cold methanol (5 min),
278 then with Triton X-100 (10 ml/L in PBS, 20 min), and
279 rinsed in PBS. Coverslips were immunostained for
280 TLQP peptides, and for the TLQP-21 receptors: gC1q-R
281 (Abcam, Antibody Registry: AB10675815, raised in
282 rabbit, 1:600), and C3a-R (Abcam, Antibody Registry:
283 AB2687440, raised in rabbit, 1:200–1000). A HuR
284 antibody (Santa Cruz, Antibody Registry: AB627770,
285 raised in mouse, 1:500), to label stress granules, and a
286 calnexin antibody (Sigma–Aldrich, Antibody Registry:
287 AB2069152, raised in mouse, 1:300), to label
288 endoplasmic reticulum (ER), were used in double-
289 immunostaining with the TLQP antiserum. Cell nuclei
290 were counterstained with bisBenzimide (Hoechst 33342,
291 0.5 µg/ml).

292 TLQP peptide/s antiserum

293 The guinea-pig primary antiserum to TLQP peptides,
294 specific for their common N-terminal portion, previously
295 described in detail (Brancia et al., 2005) was extensively
296 used in different organs and tissues (Cocco et al., 2007,
297 D'Amato et al., 2008, 2015; Brancia et al., 2010; Noli
298 et al., 2014; Noli et al., 2017). Briefly, a synthetic peptide
299 corresponding to rat VGF_{556–564}, with the addition of a C-
300 terminal cysteine residue, was conjugated *via* its C-
301 terminus to keyhole limpet hemocyanin (KLH), and used
302 for immunizations. See ELISA and immunohistochemistry
303 sections (below), for specificity controls relevant to its use
304 in each method.

305 ELISA

306 Competitive ELISA was carried out as previously
307 described in detail (Cocco et al., 2007), and the character-
308 ization of the TLQP assay are summarized in Table 1,
309 while calibration curve is shown in Fig. 1. Briefly, multiwell
310 plates (Nunc ThermoScientific, Milan, Italy) were coated
311 with the relevant synthetic peptide, hence treated with
312 PBS containing normal donkey serum (90 ml/L), aprotinin
313 (20 nmol/L), and EDTA (1 g/L) for 2 h. Primary incuba-
314 tions (3h) were carried out in duplicate, using TLQP
315 (1:5k), NERP-1 (1:160 k; Cocco et al., 2007), NAPP
316 (1:100 k; D'Amato et al., 2015) as well as N-terminus
317 and C-terminus (both 1:12 k; Cocco et al., 2010) antisera
318 followed by biotinylated secondary antibodies (Jackson,
319 West Grove, PA, Antibody registry: AB2340451; 1:10 K,
320 1 h), streptavidin-peroxidase conjugate (Biospa, Milan,
321 Italy, 30 min), and tetramethylbenzidine substrate (TMB
322 X-traKem-En-Tec, Taastrup, Denmark, 100 ml/well).
323 Reaction was stopped with HCl (1 mol/L) and optical den-
324 sity was measured at 450 nm using a multilabel plate
325 reader (Chameleon: Hidex, Turku, Finland). Recovery of
326 synthetic peptide (same used for immunization, plate
327 coating and measurement standard) added to plasma,
328 or to tissue samples at extraction was > 85%.

329 Gel chromatography

330 Plasma samples (human: 2 ml, or a pool from control
331 mice: 1 ml), as well as extracts of spinal cord (pooled
332 from control mice: 1.6 ml), NSC-34 cells (2 ml) and

333 fibroblasts (1.2 ml) were individually loaded onto a
334 Sephadex G-50S column (Sigma–Aldrich, 2 cm² × 1 m).
335 The column was equilibrated with ammonium
336 bicarbonate solution (50 mmol/L in H₂O) and eluted with
337 the same buffer (about 0.3 ml/min, using a membrane
338 pump running at 5 impulses/min, –4 °C). The column
339 was calibrated using a kit (MVG70, Sigma–Aldrich)
340 containing the following molecular weight markers:
341 bovine albumin (66 kDa), carbonic anhydrase (29 kDa),
342 cytochrome c (12.4 kDa), and aprotinin (6.5 kDa).
343 Collected fractions (3 ml) were reduced in volume using
344 a Vacufuge Concentrator (Eppendorf, Milan, Italy) and
345 assessed by ELISA. Experiments were carried out in
346 duplicate, or in triplicate, depending on sample
347 availability. Overall recovery of loaded immunoreactive
348 material/s resulted in an 81–102% range.

Detection of TLQP peptides in tissues and cells

349 TLQP antiserum (1:600–1:800) was diluted with PBS
350 containing normal donkey serum (30 ml/L, from a pool
351 of > 5 animals) and NaN₃ (0.5 g/L), with the addition of
352 normal mouse serum (30 ml/L: mouse tissue sections
353 only). Primary incubations were carried out at room
354 temperature, either overnight (16 h: mouse spinal cord
355 sections), or for 4 h (fibroblast and NSC-34 cell
356 cultures). For double-labeling, the relevant primary
357 antibodies were mixed and similarly incubated (see
358 specific part). Sites of primary immune reaction were
359 revealed using secondary IgG preparations absorbed
360 against serum proteins from multiple species (Jackson
361 Immunoresearch Laboratories, West Grove, PA, USA),
362 at a 2–10 mg/L concentration (in PBS, 1 h at room
363 temperature). As appropriate, either of the following was
364 used (1:200–300): (a) Cyanin 3.18-conjugated donkey
365 anti-guinea pig IgG (Antibody registry: AB2340460), (b)
366 Cyanin 3.18, or Alexa488-conjugated anti-mouse IgG
367 (Antibody registry: AB2340460 and AB2341099,
368 respectively), (c) a mixture of “a” and “b” above, (d)
369 Cy3-conjugated anti-rabbit IgG (Antibody registry: AB
370 2307443) (e) Alexa488-conjugated donkey anti-sheep
371 IgG (Antibody registry: AB 2340754). Routine controls
372 included: substitution of each antibody layer, in turn,
373 with PBS; the use of pre-immune, or non-immune sera;
374 the use of inappropriate secondary antibodies. Pre-
375 absorption of the TLQP antiserum with the relevant
376 (unconjugated) peptide (up to 100 mmol/L) resulted in
377 virtually complete prevention of the corresponding
378 labeling. Slides were coverslipped, and culture
379 coverslips were mounted on slides, using Glycerol–PBS
380 (1:2) containing NaN₃ (0.2 g/L). Preparations were
381 observed and photographed using a BX51 fluorescence
382 microscope (Olympus, Milan, Italy) equipped with a Fuji
383 S3 Pro digital camera (Fujifilm, Milan, Italy).
384

Western blot of TLQP-21 receptors

385 NSC-43 cell preparations were lysed in 2% sodium
386 dodecyl sulfate (20 g/L, min), and a sample (10 µl) was
387 set aside to assess protein concentration (BCA assay,
388 Thermo Scientific). Loading buffer (75 mmol/L tris–
389 hydrogen chloride buffer, pH 6.8, containing 200 ml/L
390

Table 1. VGF assay characterization

Assay	Peptide	IC ₅₀	CV1 %	CV2 %	CR %
TLQP	rVGF ₅₅₆₋₅₆₄ ¹	8	2–3	7–3	100
	rVGF ₅₅₅₋₅₆₄ (R-TLQPPASSR) [*]				3.5
	rVGF ₅₅₇₋₅₆₄ (-LQPPASSR)				20
	rVGF ₅₅₆₋₅₆₅ (TLQP11)				122
	rVGF ₅₅₆₋₅₇₆ (TLQP21)				183
	hVGF ₅₅₄₋₅₇₇ (TLQP24)				65

IC₅₀: concentration of peptide producing 50% inhibition of the maximum signal (picomoles/milliliters); CV1 and CV2: intra- and inter-assay variation, respectively; r: rat; h: human ¹“reference” peptide used for immunization, plate coating, and standard. ^{*}Arginine (R): residue added at the peptide N-terminus, to mimic its extended sequence within the VGF precursor. The cross-reactivity (CR) of each peptide is expressed compared to the “reference” peptide, a > 100% reactivity is indicated for the authentic TLQP-21 that is more reactive compared to the reference one. CV1: mean values of six different known concentrations of TLQP calibrators (500 pmol/ml, 50 pmol/ml, 5 pmol/ml, 0.5 pmol/ml, 0.05 pmol/ml, 0.005 pmol/ml; 8 replicates). CV2: three known calibrators (50 pmol/ml, 5 pmol/ml, 0.5 pmol/ml; 10 independent experiments, in duplicate).

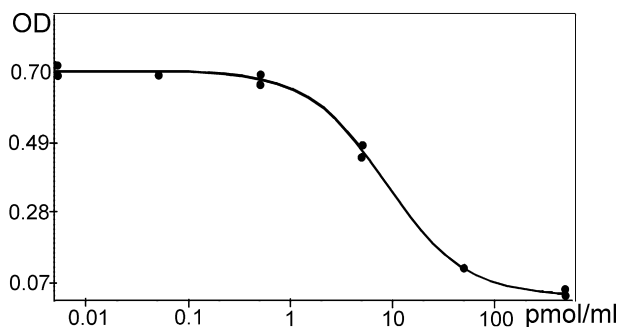


Fig. 1. Calibration curve. The standard curve was obtained using a range of concentrations of the “reference” peptide in solution (VGF₅₅₆₋₅₆₄) and a fixed amount of the same peptide onto the well, competing for the TLQP antibody, OD: optical density; pmol/ml: picomoles/milliliters.

glycerol, 0.4 g/L% SDS, 5% β-mercaptoethanol, 0.001% bromophenol blue) was added to the extract, hence tubes were heated in a vigorously boiling water bath (3 min). Samples (containing about 15 μg proteins each) were loaded onto 4–20% gradient SDS (sodium dodecyl sulfate)–polyacrylamide gels and blotted onto polyvinylidene fluoride membranes (Hybond-P, Amersham). Membranes were blocked with 5% non-fat dry milk (50 g/L, 1 h, in PBS) and incubated overnight (16 h, at 4 °C) with either of the TLQP-21 receptor antibodies (see above: NSC-34 cell cultures). On the following day, membranes were incubated with horseradish-peroxidase-conjugated anti-rabbit IgG (Invitrogen, Life Technologies, 1:5000, 1 h), hence revealed using a chemiluminescent substrate (Euroclone, SpA, Pero, Milan). A rabbit anti-actin antibody (Sigma–Aldrich, Antibody Registry: AB476697, 1:1000) was used to confirm an equal protein loading. Runs were carried out in triplicate in different days.

Statistical analyses

Statistical analyses were carried out using the Statistix software. For each experimental set, the normality of data distributions was preliminary checked using the Goodness-of-fit test. Resulting *p* values were > 0.05 in all cases, hence the following parametric tests were applied. In case of unequal variance, the Welch *t*-test (*t_w*-test) was carried out, otherwise the two-tailed

Student *t*-test with pooled variances was applied. Linear regression analysis was used to estimate possible correlations between plasma TLQP peptides, versus ALSFRS-R rating or the patients’ age. In all cases, *p*-values < 0.05 were deemed significant.

RESULTS

TLQP peptides in human

In plasma, levels of TLQP peptide immunoreactivity were roughly 80–90 pmol/ml in control subjects. A distinct reduction in plasma TLQP peptides was seen in ALS patients (Fig. 2A), already in the early stage (mean ± E S, controls: 87.2 ± 4.3; patients: 75.1 ± 4.0, *t_w*-test: *p* < 0.05, DF = 65.4,) as also in the late stage (patients: 73.5 ± 3.8, *t_w*-test: *p* < 0.05, DF: 57.3). Data are expressed as percentage of the control samples (100%). In gel chromatography, the following profile of TLQP immunoreactivity was revealed (Fig. 2B): (i) a major peak at a ~7- to 8-kDa elution position compatible with TLQP-62 (c) (ii) a broad peak in the ~6.5- to 4-kDa region probably corresponding with the TLQP-42 and 30 forms (d–e), and a lower peak at ~2- to 3-kDa compatible with TLQP-21 (f). Two larger forms were also found close to the void volume, at about 66- and 14- to 15-kDa elution positions may compatible to the VGF precursor (peak “a”) and NAPP-129 (peak “b”), respectively, both including the internal TLQP sequence. The sequences of the above TLQP peptides are summarized in Fig. 3. No correlation was found between patients’ plasma TLQP peptide levels and their corresponding ALSFRS-R score, age, or sex (Fig. 2C–E). In fibroblasts (Fig. 2F–I) a significant reduction in TLQP peptide/s immunoreactivity (pmol/μg; controls: 0.35 ± 0.04, ALS: 0.24 ± 0.02, *t*-test: *p* < 0.05, DF = 19) was shown in culture extracts from ALS patients compared to controls (Fig. 2F). TLQP peptide/s immunoreactivity was revealed in a region of cytoplasm close to the nucleus, *bona fide* the Golgi area, as previously shown (Brancia et al., 2016) and in agreement with the role of VGF as precursor of secretory products (Brancia et al., 2005). In both ALS patients and controls (Fig. 2G,H; respectively) cytoplasmic stress granules appeared after SA treatment as previously reported (Orrù et al., 2016). Such granules were not labeled by the TLQP antibodies (Fig. 2I). The molecular forms seen

6

C. Brancia et al. / Neuroscience xxx (2018) xxx–xxx

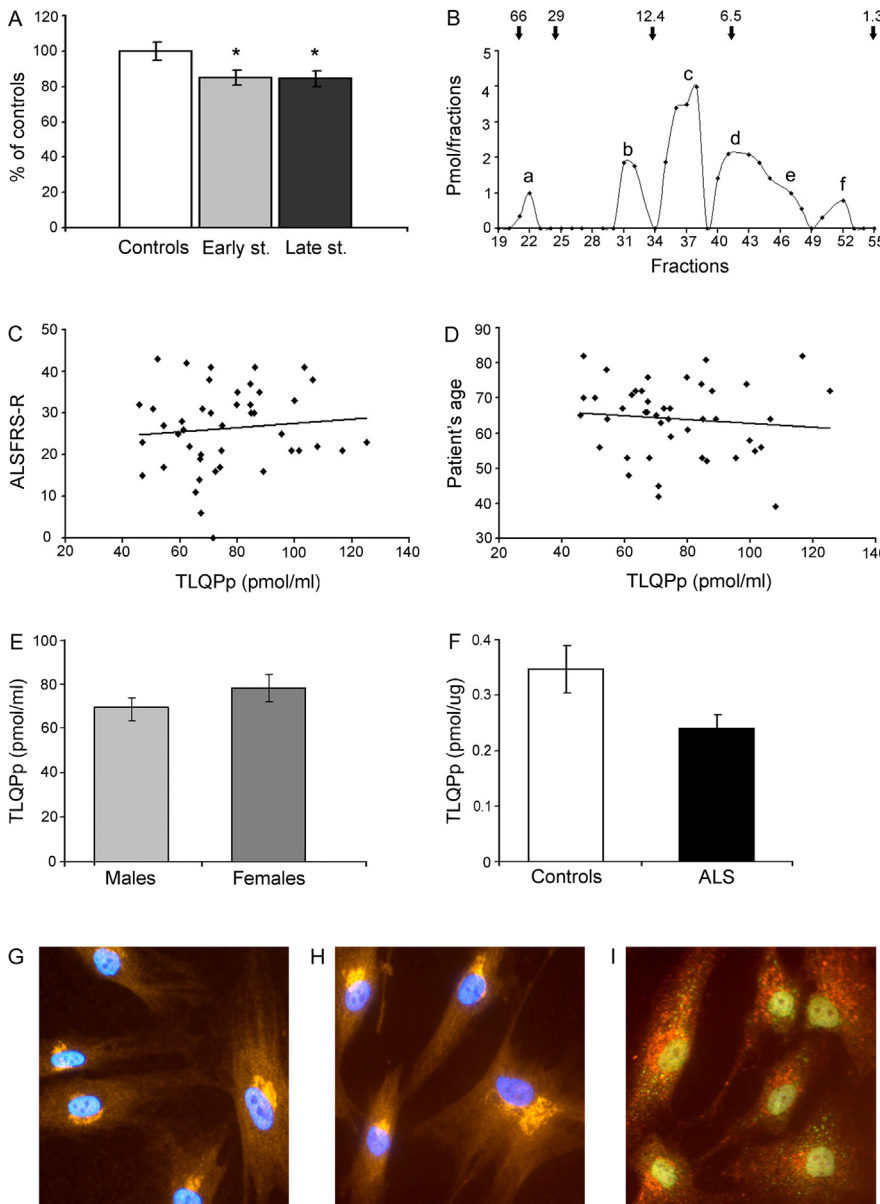


Fig. 2. TLQP peptides in human. Plasma levels of TLQP peptides (A). The levels of TLQP peptides in the early and late stage of the ALS patients ($n = 25$ and 19 , respectively) are both reduced, when compared with the controls ($n = 46$); percentage of reduction: 14 and 16 , early and late stage, respectively, t -test: $p < 0.05$. Data are expressed as percentage of the control samples (100%). Chromatographic analysis coupled with ELISA (B). The following molecular forms are recognized by the TLQP-antiserum: a. ~ 66 kDa, probably the VGF precursor; b. ~ 15 kDa compatible to NAPP-129, as well as: c. ~ 7 – 8 kDa, d–e. ~ 6.5 – 4 kDa, f. ~ 2 – 3 kDa, compatible to TLQP-62, 42, 30 and 21, respectively. Arrows in the top indicates the molecular weight markers, pmol: picomoles. ALS Functional Rating Scale Revised (ALSFRS-R) vs. TLQP peptides levels (C). There is not a statistically significant linear relationship ($p \leq 0.427$, $R = 0.124$) between TLQP peptides levels and the ALSFRS-R values; pmol/ml: picomoles/milliliter. Patient's ages vs. TLQP peptides levels (D). We observe a no statistically significant linear relationship ($p \leq 0.507$; $R = 0.103$) between TLQP peptides levels and patient's ages. TLQP peptides levels in female and male ALS patients (E). A no significant difference is found between males and females ALS patients ($p > 0.05$). TLQP in fibroblasts (F–I). TLQP peptides are reduced (F) in naive ALS patient-derived cells ($n = 4$) compared to the corresponding controls ($n = 3$; $\sim 31\%$ of controls; t -test: $p < 0.05$) pmol/ μ g: picomoles/micrograms. TLQP peptides are present in specific cytoplasm structures, probably the Golgi area, in cells from controls as well as ALS patients (G and H, respectively; red-orange, Cy3), either before (H) or after the treatment with SA (I), that produces visible stress granules (revealed with anti HuR, green, Alexa-488). The nuclei are revealed in Blue (Hoechst 33342). (For interpretation of the references to color in this figure legend, the reader is referred to the web version of this article.)

upon gel chromatography were broadly comparable to those found in plasma (data not shown).

TLQP peptides in mice

In the cervical spinal cord of wild-type mice of all ages studied, TLQP peptides were well represented in large- and medium-sized perikarya in laminae VIII and IX, the majority surrounded by the VACHT staining, hence identified as motor neurons (Fig. 4A, white arrows) while their levels (through ELISA) were in a range of 100 – 250 pmol/g. Instead, in the mutant mice, the TLQP immunoreactivity was significantly decreased, through both IHC (Fig. 4A) and ELISA in the pre-symptomatic stage (158.7 ± 15.1 and 46.6 ± 20.4 , wild type vs. SOD1, t -test: $p < 0.005$, $DF = 9$), remaining down regulated up to the late stage (WT: 186.8 ± 10.6 , SOD1: 153.5 ± 19.9 , t -test: $p < 0.05$, $DF = 10$) (Fig. 4B). Lumbar and cervical spinal cords were analyzed in parallel showing similar immunostaining profiles in both IHC and ELISA. The molecular forms recognized by the TLQP antiserum were comparable to those observed in human samples, including peaks compatible with TLQP-62,-42,-30,-21 (peaks c – f) and the two peaks, “a” and “b”, may be compatible with the VGF precursor and NAPP-129, respectively (Fig. 4C). In all wild-type mice, plasma concentrations of TLQP peptides ranged between 170 and 200 pmol/ml, while they were significantly decreased in SOD1-mutant mice at the pre-symptomatic stage (WT: 170.5 ± 17.8 , SOD1: 125.7 ± 8.8 , t -test: $p < 0.05$, $DF = 10$), remaining reduced in the late stage (WT: 171.5 ± 9.8 , SOD1: 132.3 ± 12.1 , t -test: $p < 0.05$, $DF = 10$) (Fig. 4D). Gel chromatography applied to the mouse plasma revealed similar forms observed in human and mouse spinal cord hence it was not shown.

TLQP peptides and NSC-34 cells

TLQP immunoreactivity was found in the growth cones and axons of NSC-34 cells, as well as in their cytoplasm in a para-nuclear location suggestive of its abundance in the *bona fide*

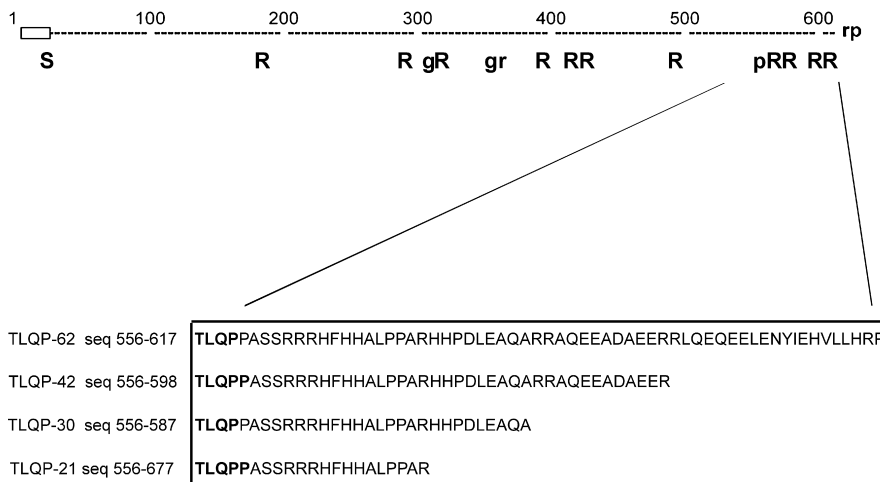


Fig. 3. TLQP sequences. The different sequences of the putative TLQP peptides are described.

518 Golgi area (Fig. 5A left panel). No co-localization was
 519 found with markers of the ER (data not shown). Upon
 520 treatment with SA, to induce oxidative stress, cells
 521 mostly lost their axons and growth cones changing to a
 522 round shape while TLQP peptides maintained their
 523 cytoplasmic localization (Fig. 5A, middle panel). No
 524 TLQP immunoreactivity was detected in stress granules
 525 (Fig. 5A, right panel). A significant decrease in TLQP
 526 peptides content (pmol/ μ g total protein; Fig. 5B) was
 527 found in SA-treated cells (naïve: 0.199 ± 0.04 , treated:
 528 0.094 ± 0.01 , t_{test} : $p < 0.05$, DF = 9). Addition of
 529 synthetic TLQP-21 (1 nmol/ml) to culture media of SA-
 530 treated cells significantly increased cell viability,
 531 compared to the SA treatment only (82.5% vs. 74.7%,
 532 $p < 0.05$; Fig. 5C). Several VGF-derived peptides were
 533 measured in naïve and SA-stressed cells. Further to
 534 TLQP peptides, these included NERP-1, NAPP and
 535 APGH peptides, as well as VGF N-terminus- and C-
 536 terminus-related peptides. Only TLQP and NERP-1
 537 peptide/s showed a significant change (reduction) in
 538 stressed cell cultures, hence were tested. However,
 539 addition of synthetic NERP-1 to the cell culture medium
 540 did not result in any detectable change in cell viability
 541 (data not shown). When we used the antibodies against
 542 the two TLQP receptors, the gC1q-R antibody showed a
 543 labeling in the nucleus with a feeble immunostaining into
 544 the cytoplasm (Fig. 5D), as expected (Soltys et al.,
 545 2000) while a weak staining only was revealed for C3a-
 546 R. The presence of gC1q-R (predicted molecular weight:
 547 33 kD) was confirmed by western blot analysis (Fig. 5E).
 548 NSC-34 extracts revealed approximately the same MW
 549 forms observed in human and mouse samples, hence they
 550 were not shown.

DISCUSSION

552 We demonstrate here a downregulation of TLQP peptides
 553 in both stressed NSC-34 cells and untreated fibroblast
 554 cultures from ALS patients, as well as in motor neurons
 555 of SOD-1 mice before the onset of significant muscle
 556 weakness. In plasma, TLQP peptides were also
 557 reduced from the early clinical stages in ALS patients,
 558 and so were in the earliest stage studied in SOD-1 mice

(pre-symptomatic stage). Hence, plasma TLQP peptides may have a value as possible biomarkers in the screening or diagnosis of suspected ALS patients.

TLQP peptides as blood biomarkers

The identification of potential biomarkers sensitive to the progression of disease is one of the present goals of ALS research. In SOD-1 mice, the reduction in TLQP peptide/s we observed in both plasma and motor neurons at the earliest, pre-symptomatic stage suggests that plasma changes may not only parallel, but also reflect early changes occurring in motor

neurons. Hence, peptides of the overall TLQP family may show promise as indicators for early diagnosis of ALS. In fact, measurement of most neurotrophic factors, including BDNF (Tremolizzo et al., 2016), failed to selectively detect ALS patients and changes at an early phase (Turner et al., 2009). In a previous study, we revealed changes in peptides derived from a different part of VGF, namely the region encompassing the C-terminal end of the VGF precursor (Brancia et al., 2016). VGF C-terminus peptides also showed significant changes in ALS patients, but only at the advanced clinical stage (Brancia et al., 2016). Hence, it is conceivable that other VGF-derived peptides, including those related to the VGF C-terminus, may decrease upon an extensive neuronal damage, while TLQP peptides are reduced at an earlier stage of initial cellular damage or breakdown. While further studies will be required, with the precise identification of the molecular forms involved, one might suggest that TLQP-21 and other related peptides, i.e., TLQP-62, could be most prominently involved in the overall changes found in the present paper. The TLQP-62 peptide, deserves a special mention, because, since it extends from the TLQP sequence to the full C-terminus of the VGF precursor, it is also recognized and measured by VGF C-terminus assay (Brancia et al., 2016). Moreover, since the Sardinian population has a high predominance of TARDBP mutation (Chiò et al., 2011), as reflected in our cohort of patients, we were not able to study any correlation between TLQP levels and specific ALS mutation/s. While future studies will be done by us to investigate if the reduction in TLQP peptides is peculiar for ALS, schizophrenia induced by phencyclidine has not produced any TLQP changes in the rat blood (Noli et al., 2017).

TLQP peptides are reduced in ALS tissues

TLQP peptides were reduced in spinal cord motor neurons of SOD1-G93A mice, in SA-stressed NSC-34 cells, as well as in fibroblast cultures from ALS patients. Interestingly, the latter patients showed a TARDBP mutation, which has also been proposed to induce cell

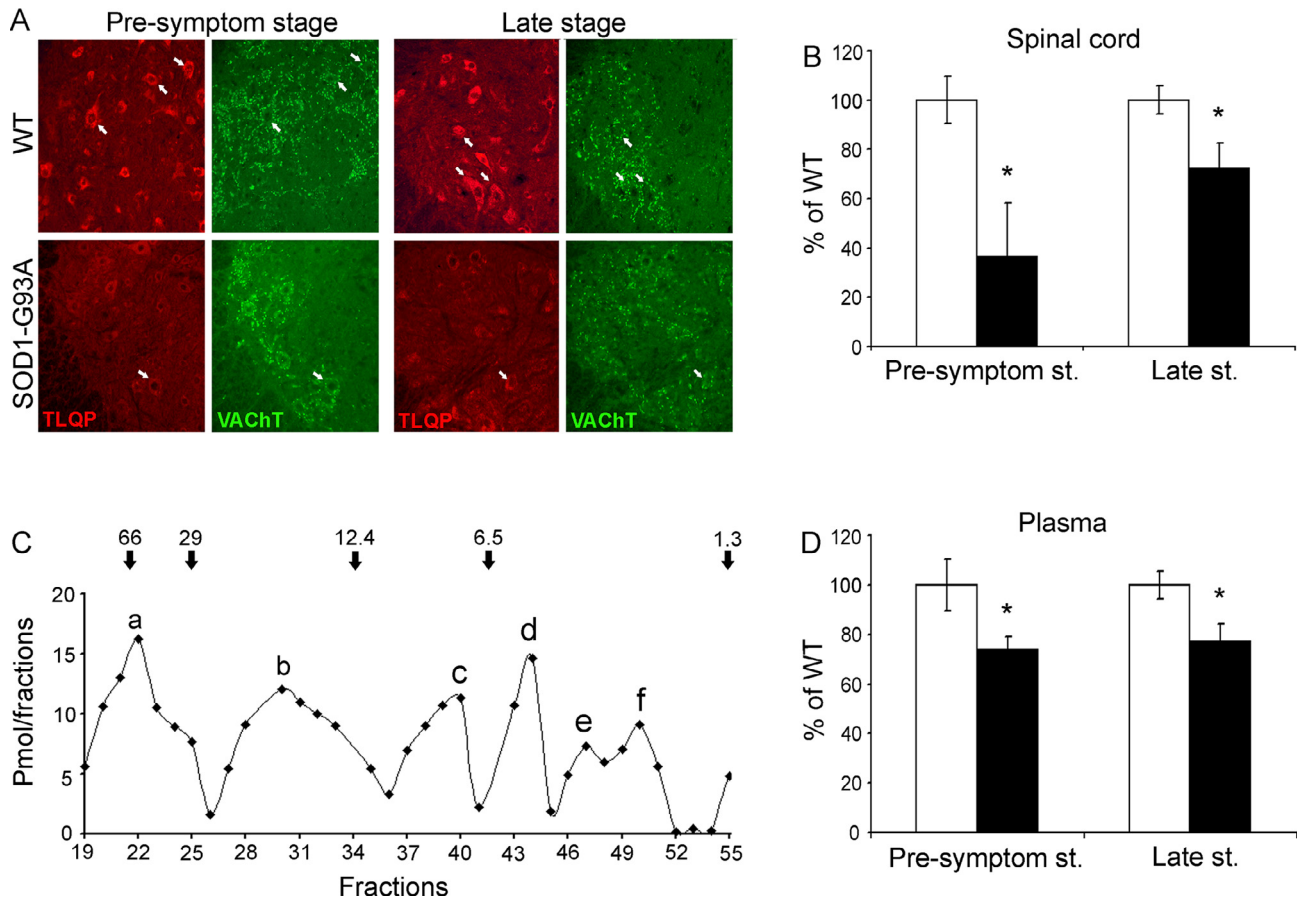


Fig. 4. TLQP peptides in mice. TLQP peptides in cervical motor neurons (A). TLQP peptides immunoreactivity (Cy3, red) is localized in a large number of perikarya of the ventral horns in wild-type mice in the age of the pre-symptomatic and late stage of transgenic mice. These cell bodies are identified as motor neurons using VAcHT antibody (Alexa-488, green). Instead, in the SOD1-G93A mice, the TLQP immunoreactivity is weak visible in a minor number of cells already in the pre-symptomatic stage and remains reduced also in the late stage ($n = 3$ per genotype). Levels of TLQP peptides in cervical spinal cord (B). TLQP levels are significantly decreased in mutant mice (vs the corresponding wild type) already in the pre-symptomatic phase (percentage of decrease: about 70%; $p < 0.005$) as well as in the late stage (18%; $p < 0.05$). Data are expressed as percentage of the control samples (100%), $n = 7$ per genotype. Chromatography analysis coupled with ELISA in spinal cord (C). Different molecular forms are recognized by the TLQP antiserum: a. ~66 kDa, compatible to the VGF precursor; b. ~15 kDa compatible to NAPP-129, and the peaks: c. ~7–8 kDa, d. ~5 kDa, e. ~3 kDa, and f. ~2 kDa, compatible to TLQP-62, 42, 30 and 21, respectively. Arrows in the top indicates the molecular weight markers; pmol:picomoles. Levels of TLQP peptides in plasma (D). TLQP levels are significantly decreased in mutant mice vs wild type already in the pre-symptomatic phase (26%; $p < 0.05$) as well as in the late stage (23%; $p < 0.05$). Data are expressed as percentage of the control samples (100%), $n = 7$ per genotype. (For interpretation of the references to color in this figure legend, the reader is referred to the web version of this article.)

617 death through oxidative stress (Duan et al., 2010; Braun
618 et al., 2011; Zhan et al., 2015). Altogether, TLQP pep-
619 tide/s change we observed probably occurred in connec-
620 tion with oxidative stress and ensuing pathophysiological
621 mechanisms. This way, the TLQP alterations occurring
622 in the spinal cord of pre-symptomatic SOD1 mice may
623 be relevant part of, or respond to the early modifications
624 triggering the waterfall of events that cause motor neuron
625 degeneration. It is worth noting that TLQP peptides were
626 localized in the *bona fide* Golgi area as well as in growth
627 cones and axons (Chevalier-Larsen and Holzbaaur, 2006).
628 Golgi fragmentation has been shown to be associated
629 with ALS hallmarks, and to occur at an early, preclinical
630 stage in both ALS patients (Maruyama et al., 2010), and
631 SOD1 mice (Vlug et al., 2005; Van Dis et al., 2014). In
632 the same mice, defects in retrograde transport, from the
633 muscle cells to the cell body of motor neurons, have been
634 suggested to be one of the earliest visible alterations
635 (Ligon et al., 2005).

TLQP-21 protects neuronal cells from oxidative stress

636 We here reported that the TLQP peptides, localized in the
637 cytoplasm and growth cones/axons of the NSC-34 cells,
638 decreased in response to oxidative stress, while the
639 TLQP-21, when added in the medium, is able to protect
640 the cells from the death. The other VGF peptides tested
641 in the stressed NSC-34 cells were not reduced, or, if
642 they were, did not protect the cells from the death (as in
643 the case of the NERP-1). Since the presence of both
644 TLQP peptides and gCq1-R within the NSC-34 cells, we
645 could speculate that the neuroprotection could be due to
646 mechanisms linked to their relationship. Actions of
647 TLQP-21 via the gC1q-R receptor have been shown to
648 be implicated in hypersensitivity in the spinal cord dorsal
649 horn (Chen et al., 2013). The gC1q-R is a ubiquitous pro-
650 tein of 33 kDa initially identified and characterized as a
651 receptor for the globular heads of the complement activa-
652
653

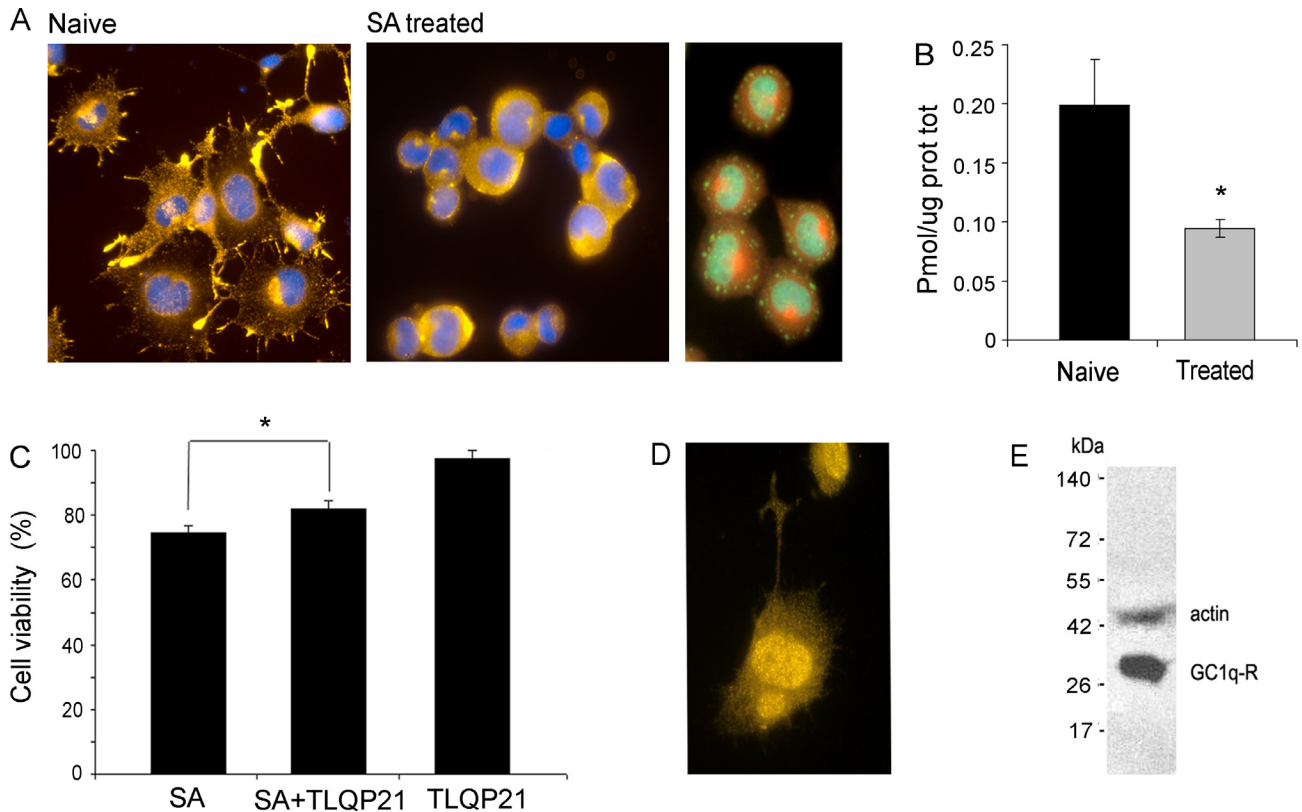


Fig. 5. TLQP peptides in NSC-34 cells. TLQP immunolocalization (A). TLQP peptides (Cy3, red-yellow) are found within the cytoplasm, probably in the Golgi area as well as in the axons and growth cones (left panel). When treated with Sodium Arsenite (SA), the cells lose their growth cones changing to a round shape (nucleus revealed in Blue: Hoechst 33342) and TLQP peptides are present exclusively within the cytoplasm (middle panel) and not visible in the stress granules (revealed with anti HuR, ALEXA488, green; right panel). TLQP levels (B). A significant TLQP peptides decrease is seen (B) in the SA-treated compared to the naïve cells (about 53%, $p < 0.05$). Pmol/ug prot tot: picomoles/micrograms of total protein. MTT viability test (C). The NSC-34 viability increases when the cells are treated with SA together with TLQP-21, compared to the treatment with the SA only (about 83% vs. 75%, $p < 0.05$). TLQP-21 alone is not able to produce any effect. The gC1q-R immunoreactivity (D,E). The gC1q-R antibody stains the nucleus as well as weakly the cytoplasm (D, Cy3 red-yellow), and also labeled a form of about 31–33 kDa revealed through Western blot (E). (For interpretation of the references to color in this figure legend, the reader is referred to the web version of this article.)

tion component C1q (Ghebrehwet et al., 1994) and involved in the inflammatory response (Peerschke and Ghebrehwet, 2007). In spinal cord motor neurons of SOD1 mice, it was found to be detectable before the appearance of the clinical symptoms (Heurich et al., 2011) with a major expression at the late stage (Lee et al., 2013). TLQP-21 has been previously reported, as mentioned, to prevent apoptosis induced by oxidative stress in both human (Zhang et al., 2013) and rat cells (Severini et al., 2008). All together these pieces of evidences highly suggest an involvement of TLQP-21–gC1q-R complex in the increased cell viability that we reported here, none the less, studies are warranted to investigate TLQP-21 activity on motor neurons in a variety of conditions. The gC1q-R is also expressed in fibroblasts (Bordin and Costa, 1998), where it might exert a protective action against oxidative stress (McGee and Baines, 2011). Hence, fibroblast cultures may be a further means to address the mechanisms implicated in TLQP-21 bioactivity, and its possible value in ALS.

Collectively, our study suggests that the TLQP family, including both TLQP-21 and TLQP-62, respond early to oxidative stress, and could be of value as a biological diagnostic index for ALS. The TLQP-21 peptide might be of some relevance to prevent or reduce motor

neuron death. Further studies may be of interest, to address the possible relevance of TLQP peptides other than TLQP-21. TLQP-62 has so far better studied, and has been shown to have a role in neurogenesis (Thakker-Varia et al., 2014). Interestingly, in ALS patients, where impaired glucose tolerance has been reported (Sun et al., 2015), certain metabolites modulated in plasma are indicative of alterations in both mitochondrial activity and carbohydrate/lipid metabolism associated with neuronal changes (Lawton et al., 2012). Since TLQP-21 is a metabolic peptide acting on energy and lipolysis mechanisms (Bartolomucci et al., 2006), and TLQP-62 is a hypoglycemic agent (Petrocchi-Passeri et al., 2015), we could speculate that both peptides could be possibly involved in the energy mechanisms that contribute to motor neuron degeneration (Dupuis et al., 2004). In conclusion, although currently there are no applicable blood diagnostic tests and pharmacological treatments for ALS, research on these topics may likely include the TLQP family.

AUTHORS' CONTRIBUTION

CB, GLF: conceived and planned the study; CB, BN, RP and MB performed experiments with assistance by AB

10

C. Brancia et al. / Neuroscience xxx (2018) xxx–xxx

702 and RP; CB, BN and CC analyzed data; MB, FM and AV
703 contributed materials and analytical tools, and reviewed
704 the manuscript; CB, CC and GLF wrote the paper. All
705 authors read and approved the final version of the
706 manuscript.

ACKNOWLEDGMENTS

707
708 Sandro Orrù provided fibroblast explants, Giuseppe
709 Borghero human plasma samples. Giacomo Diaz is
710 thanked for help with statistical analyses, Barbara
711 Manconi for quality control of synthetic peptide
712 preparations by HPLC-mass spectrometry, and Valeria
713 Sogos for unceasing encouragement (all at the
714 University of Cagliari, Cagliari, Italy). Angelo Poletti
715 (University of Milan) provided the NSC-34 cell line. This
716 work was supported by: the Autonomous Region of
717 Sardinia (Sardinia PO FSE 2007-1013 funds, L.R.
718 7/2007); NeuroCare onlus; Interdisciplinary Human
719 Movement and Rehab Research Laboratory (HuMoRe).

CONFLICTS OF INTEREST

720
721 Authors declare no conflict of interest that could prejudice
722 the impartiality of this scientific work.

REFERENCES

723
724 Aguilar E, Pineda R, Gaytán F, Sánchez-Garrido MA, Romero M,
725 Romero-Ruiz A, Ruiz-Pino F, Tena-Sempere M, Pinilla L (2013)
726 Characterization of the reproductive effects of the VGF-derived
727 peptide TLQP-21 in female rats: *in vivo* and *in vitro* studies.
728 *Neuroendocrinology* 98:38–50.
729 Bartolomucci A, La Corte G, Possenti R, Locatelli V, Rigamonti AE,
730 Torsello A, Bresciani E, Bulgarelli I, Rizzi R, Pavone F, D'Amato
731 FR, Severini C, Mignogna G, Giorgi A, Schininà ME, Elia G,
732 Brancia C, Ferri GL, Conti R, Ciani B, Pascucci T, Dell'Omo G,
733 Muller EE, Levi A, Moles A (2006) TLQP-21, a VGF-derived
734 peptide, increases energy expenditure and prevents the early
735 phase of diet-induced obesity. *Proc Natl Acad Sci U S A*
736 103:14584–14589.
737 Behnke J, Cheedalla A, Bhatt V, Bhat M, Teng S, Palmieri A, Windon
738 CC, Thakker-Varia S, Alder J (2017) Neuropeptide VGF promotes
739 maturation of hippocampal dendrites that is reduced by single
740 nucleotide polymorphisms. *Int J Mol Sci* 18:612.
741 Bergeron C (1995) Oxidative stress: its role in the pathogenesis of
742 Amyotrophic Lateral Sclerosis. *J Neurol Sci* 129:81–84.
743 Boido M, Piras A, Valsecchi V, Spigolon G, Mareschi K, Ferrero I,
744 Vizzini A, Temi S, Mazzini L, Fagioli F, Vercelli A (2014) Human
745 mesenchymal stromal cell transplantation modulates
746 neuroinflammatory milieu in a mouse model of Amyotrophic
747 Lateral Sclerosis. *Cytotherapy* 16:1059–1072.
748 Bordin S, Costa LG (1998) Fibroblast heterogeneity of signal
749 transduction mechanisms to complement-C1q. Analyses of
750 calcium mobilization, inositol phosphate accumulation, and
751 protein kinases-C redistribution. *J Periodontol* 69:642–649.
752 Bozdagi O, Rich E, Tronel S, Sadahiro M, Patterson K, Shapiro ML,
753 Alberini CM, Huntley GW, Salton SR (2008) The neurotrophin-
754 inducible gene VGF regulates hippocampal function and behavior
755 through a brain-derived neurotrophic factor-dependent
756 mechanism. *J Neurosci* 28:9857–9869.
757 Brancia C, Nicolussi P, Cappai P, La Corte G, Possenti R, Ferri GL
758 (2005) Differential expression and seasonal modulation of VGF
759 peptides in sheep pituitary. *J Endocrinol* 186:97–107.
760 Brancia C, Cocco C, D'Amato F, Noli B, Sanna F, Possenti R,
761 Argiolas A, Ferri GL (2010) Selective expression of TLQP-21 and

other VGF peptides in gastric neuroendocrine cells and
modulation by feeding. *J Endocrinol* 207:329–341.
763
764 Brancia C, Noli B, Boido M, Boi A, Puddu R, Borghero G, Marrosu
765 F, Bongioanni P, Orrù S, Manconi B, D'Amato F, Messana I,
766 Vincenzoni F, Vercelli A, Ferri GL, Cocco C (2016) VGF
767 protein and its C-terminal derived peptides in Amyotrophic
768 Lateral Sclerosis: human and animal model studies. *PLoS ONE*
769 11(10).
770 Braun RJ, Sommer C, Carmona-Gutierrez D, Khoury CM, Ring J,
771 Büttner S, Madeo F (2011) Neurotoxic 43-kDa TAR DNA-binding
772 protein (TDP-43) triggers mitochondrion-dependent programmed
773 cell death in yeast. *J Biol Chem* 286:19958–19972.
774 Cassina V, Torsello A, Tempestini A, Salerno D, Brogioli D, Tamiazzo
775 L, Bresciani E, Martinez J, Fehrentz JA, Verdì P, Omeljaniuk RJ,
776 Possenti R, Rizzi L, Locatelli V, Mantegazza F (2013) Biophysical
777 characterization of a binding site for TLQP-21, a naturally
778 occurring peptide which induces resistance to obesity. *Biochim*
779 *Biophys Acta* 1828:455–460.
780 Cedarbaum JM, Stambler N, Malta E, Fuller C, Hilt D, Thurmond B,
781 Nakanishi A (1999) The ALSFRS-R: a revised ALS functional
782 rating scale that incorporates assessments of respiratory function.
783 BDNF ALS Study Group (Phase III). *J Neurol Sci* 169:13–21.
784 Cero C, Vostrikov VV, Verardi R, Severini C, Gopinath T, Braun PD,
785 Sassano MF, Gurney A, Roth BL, Vulchanova L, Possenti R,
786 Veglia G, Bartolomucci A (2014) The TLQP-21 peptide activates
787 the G-protein-coupled receptor C3aR1 via a folding-upon-binding
788 mechanism. *Structure* 22:1744–1753.
789 Cero C, Razzoli M, Han R, Sahu BS, Patricelli J, Guo Z, Zaidman NA,
790 Miles JM, O'Grady SM, Bartolomucci A (2016) The neuropeptide
791 TLQP-21 opposes obesity via C3aR1-mediated enhancement of
792 adrenergic-induced lipolysis. *Mol Metab* 6:148–158.
793 Chen YC, Pristerá A, Ayub M, Swanwick RS, Karu K, Hamada Y,
794 Rice AS, Okuse K (2013) Identification of a receptor for
795 neuropeptide VGF and its role in neuropathic pain. *J Biol Chem*
796 288:34638–34646.
797 Chevalier-Larsen E, Holzbaur ELF (2006) Axonal transport and
798 neurodegenerative disease. *Biochim Biophys Acta*
799 1762:1094–1108.
800 Chiò A, Borghero G, Pugliatti M, Ticca A, Calvo A, Moglia C, Mutani
801 R, Brunetti M, Ossola I, Marrosu MG, Murru MR, Floris G, Cannas
802 A, Parish LD, Cossu P, Abramzon Y, Johnson JO, Nalls MA,
803 Arepalli S, Chong S, Hernandez DG, Traynor BJ, Restagno G
804 (2011) Large proportion of Amyotrophic Lateral Sclerosis cases in
805 Sardinia due to a single founder mutation of the TARDBP gene.
806 *Arch Neurol* 68:594–598.
807 Cocco C, Brancia C, Pirisi I, D'Amato F, Noli B, Possenti R, Ferri GL
808 (2007) VGF metabolic-related gene: distribution of its derived
809 peptides in mammalian pancreatic islets. *J Histochem Cytochem*
810 55:619–628.
811 Cocco C, D'Amato F, Noli B, Ledda A, Brancia C, Bongioanni P, Ferri
812 GL (2010) Distribution of VGF peptides in the human cortex and
813 their selective changes in Parkinson's and Alzheimer's diseases.
814 *J Anat* 217:683–693.
815 D'Amato F, Noli B, Brancia C, Cocco C, Flore G, Collu M, Nicolussi P,
816 Ferri GL (2008) Differential distribution of VGF-derived peptides in
817 the adrenal medulla and evidence for their selective modulation. *J*
818 *Endocrinol* 197:359–369.
819 D'Amato F, Noli B, Angioni L, Cossu E, Incani M, Messana I, Manconi
820 B, Solinas P, Isola R, Mariotti S, Ferri GL, Cocco C (2015) VGF
821 peptide profiles in type 2 diabetic patients' plasma and in obese
822 mice. *PLoS ONE* 10(11).
823 DeJesus-Hernandez M, Mackenzie IR, Boeve BF, Boxer AL, Baker
824 M, Rutherford NJ, Nicholson AM, Finch NA, Flynn H, Adamson J,
825 Kouri N, Wojtas A, Sengdy P, Hsiung GY, Karydas A, Seeley
826 WW, Josephs KA, Coppola G, Geschwind DH, Wszolek ZK,
827 Feldman H, Knopman DS, Petersen RC, Miller BL, Dickson DW,
828 Boylan KB, Graff-Radford NR, Rademakers R (2011) Expanded
829 GGGGCC hexanucleotide repeat in noncoding region of
830 C9ORF72 causes chromosome 9p-linked FTD and ALS.
831 *Neuron* 72:245–256.

- 832 Duan W, Li X, Shi J, Guo Y, Li Z, Li C (2010) Mutant TAR DNA-
833 binding protein-43 induces oxidative injury in motor neuron-like
834 cell. *Neuroscience* 169:1621–1629.
- 835 Dupuis L, Oudart H, Rene F, Gonzalez de Aguilar JL, Loeffler JP
836 (2004) Evidence for defective energy homeostasis in amyotrophic
837 lateral sclerosis: benefit of a high-energy diet in a transgenic
838 mouse model. *Proc Natl Acad Sci USA* 101:11159–11164.
- 839 Ghebrehwet B, Lim BL, Peerschke EI, Willis AC, Reid KB (1994)
840 Isolation, cDNA cloning, and overexpression of a 33-kD cell
841 surface glycoprotein that binds to the globular “heads” of C1q. *J*
842 *Exp Med* 1(179):1809–1821.
- 843 Hannedouche S, Beck V, Leighton-Davies J, Beibel M, Roma G,
844 Oakeley EJ, Lannoy V, Bernard J, Hamon J, Barbieri S, Preuss I,
845 Lasbennes MC, Sailer AW, Suply T, Seuwen K, Parker CN,
846 Bassilana F (2013) Identification of the C3a receptor (C3AR1) as
847 the target of the VGF-derived peptide TLQP-21 in rodent cells. *J*
848 *Biol Chem* 288:27434–27443.
- 849 Heurich B, El Idrissi NB, Donev RM, Petri S, Claus P, Neal J, Morgan
850 BP, Ramaglia V (2011) Complement upregulation and activation
851 on motor neurons and neuromuscular junction in the SOD1-G93A
852 mouse model of familial Amyotrophic Lateral Sclerosis. *J*
853 *Neuroimmunol* 235:104–109.
- 854 Jethwa PH, Warner A, Nilaweera KN, Brameld JM, Keyte JW, Carter
855 WG, Bolton N, Bruggraber M, Morgan PJ, Barrett P, Ebling FJP
856 (2007) VGF-derived peptide, TLQP-21, regulates food intake and
857 body weight in Siberian hamsters. *Endocrinology* 148:4044–4055.
- 858 Lawton KA, Cudkovicz ME, Brown MV, Alexander D, Caffrey R, Wulff
859 JE, Bowser R, Lawson R, Jaffa M, Milburn MV, Ryals JA, Berry
860 JD (2012) Biochemical alterations associated with ALS.
861 *Amyotroph Lateral Scler* 13:110–118.
- 862 Lee JD, Kamaruzaman NA, Fung JN, Taylor SM, Turner BJ, Atkin JD,
863 Woodruff TM, Noakes PG (2013) Dysregulation of the
864 complement cascade in the hSOD1-G93A transgenic mouse
865 model of Amyotrophic Lateral Sclerosis. *J Neuroinflamm* 10:119.
- 866 Lewis JE, Brameld JM, Hill P, Cocco C, Noli B, Ferri G-L, Barrett PF,
867 Ebling FJ, Jethwa PH (2017) Hypothalamic over-expression of
868 VGF in the Siberian hamster increases energy expenditure and
869 reduces body weight gain. *PLoS One* 12(2):24.
- 870 Ligon LA, LaMonte BH, Wallace KE, Weber N, Kalb RG, Holzbaur EL
871 (2005) Mutant superoxide dismutase disrupts cytoplasmic dynein
872 in motor neurons. *NeuroReport* 16:533–536.
- 873 Lin WJ, Jiang C, Sadahiro M, Bozdagi O, Vulchanova L, Alberini CM,
874 Salton SR (2015) VGF and its C-terminal peptide TLQP-62
875 regulate memory formation in hippocampus via a BDNF-TrkB-
876 dependent mechanism. *J Neurosci* 35:10343–10356.
- 877 Maruyama H, Morino H, Ito H, Izumi Y, Kato H, Watanabe Y (2010)
878 Mutations of optineurin in Amyotrophic Lateral Sclerosis. *Nature*
879 465:223–226.
- 880 McGee AM, Baines CP (2011) Complement 1q-binding protein
881 inhibits the mitochondrial permeability transition pore and
882 protects against oxidative stress-induced death. *Biochem J*
883 433:119–125.
- 884 Moss A, Ingram R, Koch S, Theodorou A, Low L, Baccei M, Hathway
885 GJ, Costigan M, Salton SR, Fitzgerald M (2008) Origins, actions
886 and dynamic expression patterns of the neuropeptide VGF in rat
887 peripheral and central sensory neurones following peripheral
888 nerve injury. *Mol Pain* 4:62.
- 889 Noli B, Brancia C, D’Amato F, Ferri GL, Cocco C (2014) VGF
890 changes during the estrous cycle: a novel endocrine role for TLQP
891 peptides? *PLoS ONE* 9(10).
- 892 Noli B, Brancia C, Pilleri R, D’Amato F, Messina I, Manconi B, Ebling
893 FJ, Ferri GL, Cocco C (2015) Photoperiod regulates vgf-derived
894 peptide processing in Siberian hamsters. *PLoS ONE* 10(11).
- 895 Noli B, Sanna F, Brancia C, D’Amato F, Manconi B, Vincenzoni F,
896 Messina I, Melis MR, Argiolas A, Ferri GL, Cocco C (2017)
897 Profiles of VGF peptides in the rat brain and their modulations
898 after phencyclidine treatment. *Front Cell Neurosci* 11:158.
- 899 Orrù S, Coni P, Floris A, Littera R, Carcassi C, Sogos V, Brancia C
900 (2016) Reduced stress granule formation and cell death in
901 fibroblasts with the A382T mutation of TARDBP gene: evidence
for loss of TDP-43 nuclear function. *Hum Mol Genet* 902
25:4473–4483. 903
- Pasinetti GM, Ungar LH, Lange DJ, Yemul S, Deng H, Yuan X, Brown
904 RH, Cudkovicz ME, Newhall K, Peskind E, Marcus S, Ho L (2006)
905 Identification of potential CSF biomarkers in ALS. *Neurology* 906
66:1218–1222. 907
- Peerschke EI, Ghebrehwet B (2007) The contribution of gC1qR/p33
908 in infection and inflammation. *Immunobiology* 212:333–342. 909
- Petrocchi-Passeri P, Cero C, Cutarelli A, Frank C, Severini C,
910 Bartolomucci A, Possenti R (2015) The VGF-derived peptide
911 TLQP-62 modulates insulin secretion and glucose homeostasis. *J*
912 *Mol Endocrinol* 54:227–239. 913
- Razzoli M, Bo E, Pascucci T, Pavone F, D’Amato FR, Cero C,
914 Sanghez V, Dadomo H, Palanza P, Parmigiani S, Ceresini G,
915 Puglisi-Allegra S, Porta M, Panzica GC, Moles A, Possenti R,
916 Bartolomucci A (2012) Implication of the VGF-derived peptide
917 TLQP-21 in mouse acute and chronic stress responses. *Behav*
918 *Brain Res* 229:333–339. 919
- Renton P, Speed J, Maddaford S, Annedi SC, Ramnauth J, Rakhit S,
920 Bioarg Andrews J (2011) 1,5-Disubstituted indole derivatives as
921 selective human neuronal nitric oxide synthase inhibitors. *Med*
922 *Chem Lett* 21:5301–5304. 923
- Rizzi R, Bartolomucci A, Moles A, D’Amato F, Sacerdote P, Levi A, La
924 Corte G, Ciotti MT, Possenti R, Pavone F (2008) The VGF-
925 derived peptide TLQP-21: a new modulatory peptide for
926 inflammatory pain. *Neurosci Lett* 441:129–133. 927
- Robberecht W (2000) Oxidative stress in Amyotrophic Lateral
928 Sclerosis. *J Neurol* 247(1):11–6. 929
- Sabatelli M, Zollino M, Conte A, Del Grande A, Marangi G, Lucchini
930 M, Mirabella M, Romano A, Piacentini R, Bisogni G, Lattante S,
931 Luigetti M, Rossini PM, Moncada A (2015) Primary fibroblasts
932 cultures reveal TDP-43 abnormalities in Amyotrophic Lateral
933 Sclerosis patients with and without SOD1 mutations. *Neurobiol*
934 *Aging* 36(5). 935
- Severini C, Ciotti MT, Biondini L, Quaresima S, Rinaldi AM, Levi A,
936 Frank C, Possenti R (2008) TLQP-21, a neuroendocrine VGF-
937 derived peptide, prevents cerebellar granule cells death induced
938 by serum and potassium deprivation. *J Neurochem* 104:534–544. 939
- Soltys MJ, Kang D, Gupta RS (2000) Localization of P32 protein
940 (gC1q-R) in mitochondria and at specific extramitochondrial
941 locations in normal tissues. *Histochem Cell Biol* 114:245–255. 942
- Sun Y, Lu CJ, Chen RC, Hou WH, Li CY (2015) Risk of Amyotrophic
943 Lateral Sclerosis in patients with diabetes: a nationwide
944 population-based cohort study. *J Epidemiol* 25:445–451. 945
- Thakker-Varia S, Behnke J, Doobin D, Dalal V, Thakkar K, Khadim F,
946 Wilson E, Palmieri A, Antila H, Rantamaki T, Alder J (2014) VGF
947 (TLQP-62)-induced neurogenesis targets early phase neural
948 progenitor cells in the adult hippocampus and requires
949 glutamate and BDNF signaling. *Stem Cell Res* 12:762–777. 950
- Trani E, Giorgi A, Canu N, Amadori G, Rinaldi AM, Halban PA, Ferri
951 GL, Possenti R, Schininà ME, Levi A (2002) Isolation and
952 characterization of VGF peptides in rat brain. Role of PC1/3 and
953 PC2 in the maturation of VGF precursor. *J Neurochem* 954
81:567–574. 955
- Tremolizzo L, Pellegrini A, Conti E, Arosio A, Gerardi F, Lunetta C,
956 Magni P, Appollonio I, Ferrarese C (2016) BDNF serum levels
957 with respect to multidimensional assessment in Amyotrophic
958 Lateral Sclerosis. *Neurodegener Dis* 16:192–198. 959
- Turner MR, Kiernan MC, Leigh PN, Talbot K (2009) Biomarkers in
960 Amyotrophic Lateral Sclerosis. *Lancet Neurol* 8:94–109. 961
- Van Dis V, Kuijpers M, Haasdijk ED, Teuling E, Oakes SA,
962 Hoogenraad CC (2014) Golgi fragmentation precedes
963 neuromuscular denervation and is associated with endosome
964 abnormalities in SOD1-ALS mouse motor neurons. *Acta*
965 *Neuropathol Commun* 2:38. 966
- Vlug AS, Teuling E, Haasdijk ED, French P, Hoogenraad CC,
967 Jaarsma D (2005) ATF3 expression precedes death of spinal
968 motoneurons in amyotrophic lateral sclerosis-SOD1 transgenic
969 mice and correlates with c-Jun phosphorylation, CHOP
970 expression, somato-dendritic ubiquitination and Golgi
971 fragmentation. *Eur J Neurosci* 22:1881–1894. 972

973 Yang S, Zhang KY, Kariawasam R, Bax M, Fifita JA, Ooi L, Yerbury 986
 974 JJ, Nicholson GA, Blair IP (2015) Evaluation of skin fibroblasts 987
 975 from Amyotrophic Lateral Sclerosis patients for the rapid study of 988
 976 pathological features. *Neurotox Res* 28:138–146. 989
 977 Zarei S, Carr K, Reiley L, Diaz K, Guerra O, Altamirano PF, Pagani 990
 978 W, Lodin D, Orozco G, China A (2015) A comprehensive review 991
 979 of Amyotrophic Lateral Sclerosis. *Surg Neurol Int* 6:171.
 980 Zhan L, Xie Q, Tibbetts RS (2015) Opposing roles of p38 and JNK in
 981 a *Drosophila* model of TDP-43 proteinopathy reveal oxidative
 982 stress and innate immunity as pathogenic components of
 983 neurodegeneration. *Hum Mol Genet* 24:757–772.
 984 Zhang W, Ni C, Sheng J, Hua Y, Ma J, Wang L, Zhao Y, Xing Y
 985 (2013) TLQP-21 protects human umbilical vein endothelial cells
 994 against high-glucose-induced apoptosis by increasing G6PD
 expression. *PLoS ONE* 8(11).
 Zhao Z, Lange DJ, Ho L, Bonini S, Shao B, Salton SR, Thomas S,
 Pasinetti GM (2008) VGF is a novel biomarker associated with
 muscle weakness in Amyotrophic Lateral Sclerosis (ALS), with a
 potential role in disease pathogenesis. *Int J Med Sci* 5:92–99.

APPENDIX A

Table 1A

Table 1A. Characteristics of patients.

P#	Age	Gender	ALSFRS-R Score	Genetic mutation	Co-morbidity
1	67	M	25	TDP-43 A382T	
2	66	F	19	TDP-43 A382T	
3	81	F	30	nd	MDS
4*	39	F	22	TDP-43 A382T	
5	56	F	43	SOD1	
6*	66	F	14	TDP-43 A382T	
7	82	M	21	nd	
8	72	F	22	TDP-43 A382T	
9*	53	M	28	nd	
10*	72	M	11	C9ORF expansion	
11	48	M	26	TDP-43 A382T	
12*	64	M	27	nd	
13	56	M	41	C9ORF expansion	DVT
14	71	M	42	SOD1	
15*	55	M	21	TDP-43 A382T	
16	64	F	38	SOD1	
17	78	M	17	TDP-43 A382T	
18*	42	F	30	nd	
19	53	F	31	nd	
20	65	F	38	C9ORF72 expansion	
21	70	M	15	nd	
22*	69	M	6	TDP-43 A382T	
23	70	F	31	TDP-43 A382T	psychosis
24*	82	M	23	TDP-43 A382T	
25*	76	F	20	TDP-43 A382T	
26*	61	M	35	nd	
27	45	M	41	TDP-43 A382T	
28	53	F	25	nd	
29*	64	M	30	nd	
30	76	M	32	nd	
31*	64	M	17	nd	
32*	53	M	37	nd	
33	72	M	35	TDP-43 A382T	
34	58	M	33	ndr	
35	52	M	41	C9ORF72 expansion	
36	67	M	16	nd	K colon
37*	72	F	23	C9ORF72 expansion	
38*	74	F	32	nd	
39	67	F	21	TDP-43 A382T	Sjögren's syndrome
40	74	F	21	nd	
41*	59	F	27	nd	
42*	64	F	16	nd	
43*	63	F	0	nd	
44	65	M	32	TDP-43 A382T	Parkinsonism

* Late stage of ALS disease; nd: not determined; DVT: deep vein thrombosis; MDS: Myelodysplastic syndrome.